Fluvial processes and streamflow variability: Interplay in the scale-frequency continuum and implications for scaling

Boyko Dodov and Efi Foufoula-Georgiou

National Center for Earth-surface Dynamics and St. Anthony Falls Laboratory, Department of Civil Engineering, University of Minnesota, Minneapolis, Minnesota, USA

[1]   This paper explores the links between channel/floodplain morphometry, streamflow variability, and sediment transport across a wide range of scales and frequencies of discharge. On the basis of extensive analysis of observations from a climatologically and geologically homogeneous region in the midwestern United States, we provide evidence that streamflow statistics are significantly affected by the scale-dependent channel/floodplain interactions, which in turn are controlled by (and at the same time actively participate in defining) the dominant fluvial processes at a given scale. More specifically, we document that (1) the channel cross-sectional geometry exerts a strong control on the frequency distributions of both daily and maximum annual discharges; (2) the frequency of exceedance of bank-full discharge is scale dependent (particularly, channels draining large areas flood less often but stay overbank longer than channels draining small areas); (3) the critical area at which the variability of floods with scale changes from increasing to decreasing associates with the scale at which the fluvial regime changes from net-erosional to net-depositional and the floodplain gets well established due to its increased frequency of occupation by the flow; and (4) scaling in suspended sediment load reflects the scaling in channel and floodplain morphometry and depicts the signature of the aforementioned fluvial regime transition. The observation is made that maximum annual floods are composed of two distinct populations, one from below and one from above bank-full flows, and that the quantile at which this transition occurs depends on scale. On the basis of this observation, the notion of statistical multiscaling of floods is reexamined.

1.   Introduction

[2]   Maximum annual floods are important to hydrologists, as they form the basis of flood frequency analysis used for estimation of design events. The lack of long records for reliable estimation of extremes has always been a concern and has prompted the development of flood frequency regionalization methods by which substitution of space for time has been explored. The so-called index flood method [*Dalrymple*, 1960] was such an attempt and provided the means to assign the same probability density function (PDF) to maximum annual floods from different basins under a simple normalization by the mean annual discharge.

[3]   An important piece of work in the context of scaling of floods was that of *Gupta and Waymire* [1990], where a generalized framework for regional flood frequency analysis was proposed using a multiscaling formalism. According to this formalism, the probability distributions of maximum annual floods can be normalized by a scaling function $G(\lambda)$ (random or nonrandom) which depends on

contributing area (scale λ). If $G(\lambda)$ is a nonrandom function, a simple scaling is said to hold, which can be characterized in the following way: (1) Statistical moments form straight lines with scale in the log-log domain; (2) the coefficient of variation (CV) does not depend on scale; and (3) quantiles are log-log linear with scale with a slope that is independent of the quantile. In this framework, the index flood method is nothing more than assuming simple scaling [e.g., see *Gupta and Waymire*, 1990]. If $G(\lambda)$ is a random function, then multiscaling is assumed to hold, which obeys point 1, but the CV of the underlying distributions is a function of scale, and the log-quantiles follow nonparallel (and in general nonlinear) trends with different slopes depending on the frequency of the quantile.

[4]   Several authors [e.g., *Smith*, 1992; *Gupta et al.*, 1994] have inferred based on observations that the CV of annual maximum floods follows an increasing trend with scale up to a certain scale (called critical area A_C) after which it starts to decrease. *Gupta et al.* [1994] showed that such a behavior can be described within the multiscaling formalism which admits two distinct mathematical representations of $G(\lambda)$: one for $\lambda < 1$ (scale magnification) with decreasing variability with scale and one for $\lambda > 1$ (scale contraction) with

increasing variability with scale. Thus, for small basins ($A_0 < A < A_C$, $\lambda = A/A_0 > 1$) and large basins ($A_C < A < A_1$, $\lambda = A/A_1 < 1$), *Gupta et al.* [1994] derived theoretical expressions relating flood quantities with drainage areas for the class of log-Levy models, of which the lognormal model is a special case. According to the lognormal multiscaling model, the logarithms of flood quantiles are

$$\ln Q_p(A) = \left(\alpha^0 + \beta^0 \ln A\right) + \left(\gamma^0 + \delta^0 \ln A\right)^{1/2} z_p, \text{for } A_0 < A < A_C$$
$$(1a)$$

$$\ln Q_p(A) = \left(\alpha^1 + \beta^1 \ln A\right) + \left(\gamma^1 - \delta^1 \ln A\right)^{1/2} z_p, \text{for } A_C < A < A_1,$$
$$(1b)$$

where α^i, β^i, $\gamma^i > 0$, $\delta^i > 0$; $i = 0, 1$ are statistical parameters and z_p is the pth quantile of a standard normal distribution. A_0 and A_1 are the lower and upper bounds, respectively, of the range of contributing areas within which the scaling holds, and A_C is the critical area (reported by *Smith* [1992] to be approximately 100 km^2 in the Appalachian region) determining which statistical model applies for a given A.

[5] In a series of subsequent studies [e.g., see *Robinson and Sivapalan*, 1997; *Menabde and Sivapalan*, 2001; *Menabde et al.*, 2001; *Gupta*, 2004], attempts were made to explain the physical origin of these two scaling regimes and the scale of the break between them. More specifically, through extensive numerical simulations, *Robinson and Sivapalan* [1997] related the increasing variability of floods up to the critical area A_C to the scaling behavior of the catchment response (i.e., scaling of the ratio of storm duration to catchment response time), and the decreasing variability after that scale to the spatial scaling of excess rainfall intensity. Along the same lines, *Menabde and Sivapalan* [2001] showed that for a given rainfall duration, the flow up to a given scale is saturated (i.e., it approaches some constant discharge depending on the concentration time of the basin), while streams draining larger areas never reach saturation under the same conditions. As a result, two scaling regimes in maximum annual floods occur, one below the maximum scale at which saturation is achieved (with exponents close to 1), and one above this scale (with lower exponents).

[6] The simulation analyses performed by *Robinson and Sivapalan* [1997] and *Menabde and Sivapalan* [2001] provide useful frameworks within which to test hypotheses on the physical origins of flood scaling due to the interplay of space-time variable rainfall and river network topology. These numerical frameworks are simplified in terms of the representation of channel morphometry-streamflow relationships, namely, they consider wide rectangular cross sections and hydraulic geometry represented by power laws with constant exponents (an assumption recently challenged on both statistical and physical grounds by *Dodov and Foufoula-Georgiou* [2004a, 2004b]) and do not take into account the possible effect of overbank flows on flood wave propagation and flood statistics.

[7] To the best of our knowledge, there are no studies that explicitly consider the effect of channel-floodplain mor-

phometry on the statistics of floods in an attempt to seek a physical explanation of scaling (in terms of different scaling regimes and scaling break) as a consequence of fluvial processes. Our study is a first step in this direction. It represents an effort to understand the coupled hydrologic-geomorphologic system across a range of scales and relate the form of channels and floodplains to the variability and scaling of floods. The study is based on a comprehensive analysis of channel morphometry, on analysis of daily streamflow and maximum annual floods, on analysis of suspended sediment loads as a function of frequency of discharge and scale (upstream drainage area), and on analysis of floodplain morphometry extracted from hydrography data and verified by sedimentary deposit data near riverbanks. Some important hypotheses as to the nature of the hydrologic-geomorphologic connections as they manifest themselves at different scales and the signature they leave on the scaling of floods and suspended sediment loads are posed and tested.

[8] The flow of the paper is as follows. In section 2 we present an overview of the data used in our analysis. These data include daily flows, maximum annual floods, DEM and high-resolution hydrography data, suspended sediment load, and lithologic log data from which the depth to the bedrock is extracted. In section 3 we examine the relations between channel morphometry and streamflow variability. In particular, we provide empirical evidence for the significant effect that the channel morphometry and especially the transition from below-bank-full to overbank flow has on the probability distribution of extreme events (i.e., maximum annual floods) and long-term daily discharges (i.e., flow-duration curves). We also document that the bank-full discharge has a frequency of exceedance which depends on scale. In section 4 we show that the scale-dependent transition to overbank flow has an impact on the scaling of streamflow statistics at all frequencies from daily discharges to maximum annual floods. It also has an impact on the scaling of the hydrologic response function as inferred from an examination of the wave celerity (inverse of the flood wave propagation time) in three basins of different size and for discharges ranging from below to above bank-full. Section 5 is devoted to physical interpretations of the empirically established covariation of scaling regimes and scaling breaks in the coupled hydro-geomorphologic system. First, having established how channel morphometry affects streamflow variability, we use the concept of dominant discharge [e.g., see *Wolman and Miller*, 1960] to investigate how streamflow variability, and its dependence on scale, might affect channel geometry. Second, we offer a possible explanation for the scaling break in floods and the transition from increasing to decreasing variability with scale, in terms of a well-documented transition in the fluvial regime, from net-erosional to net-depositional. We support this hypothesis by analysis of suspended sediment load and floodplain morphometry as a function of scale. Conclusions and final remarks are presented in section 6.

2. Overview of the Area and Data Sets Used in Our Analysis

[9] The data used in this study cover a large region including southern Nebraska and Iowa, eastern Kansas,
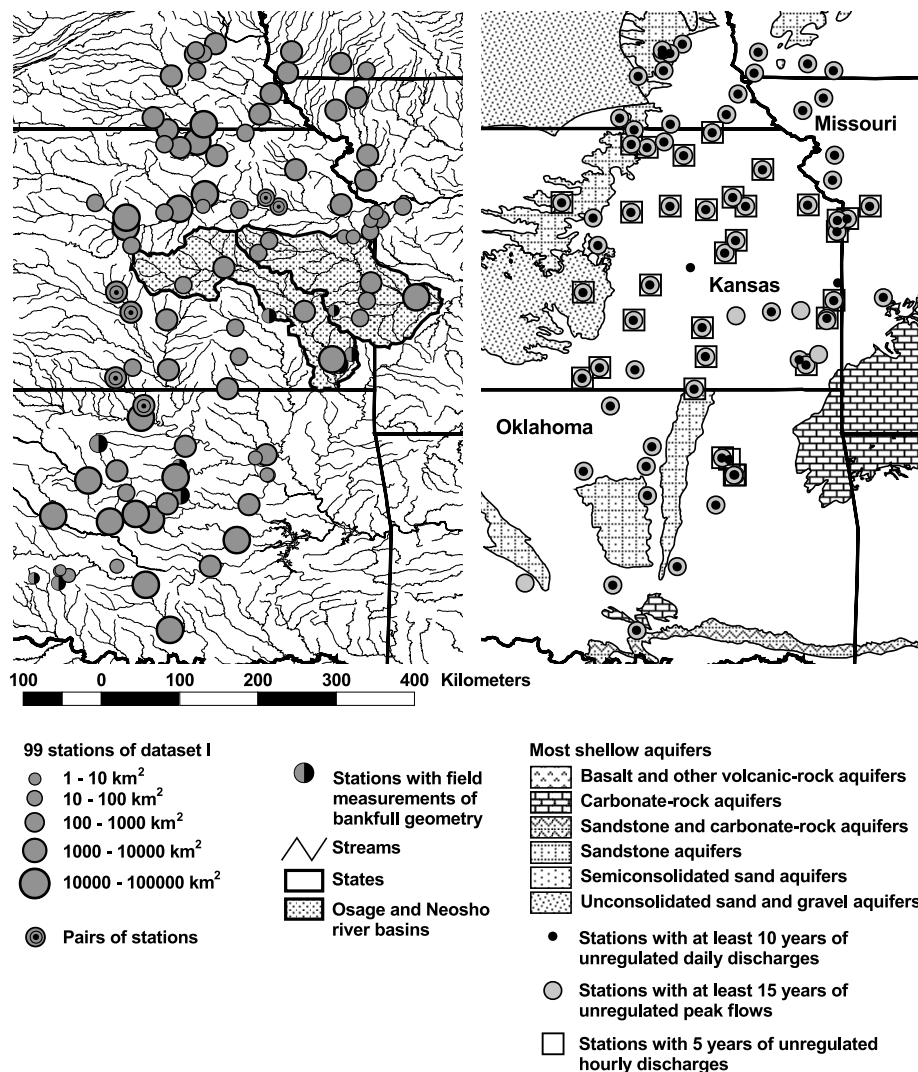
Figure 1. Locations of the 99 stations from data set I superimposed on (left) a drainage network map and (right) an underlying geology map. The shaded (Neosho and Osage River) basins are shown in more detail in Figure 2.

western Missouri, and northeastern Oklahoma. The region is characterized by similar climate (similar mean annual temperatures, 12°–17°C, and annual precipitation of 750–950 mm), similar geologic conditions (shallow top soils followed by almost impermeable shale or alternation of shale and limestone), and similar topography (in terms of elevation band and area-slope relationships). Thus the effect of climatic, geologic, and topographic heterogeneities on our analysis is assumed negligible.

2.1. Data Set I

[10] Data from 99 stations in Nebraska, Iowa, Kansas, Missouri, and Oklahoma (see Figure 1) consist of (1) independent measurements of maximum width, mean depth, cross-sectional area, mean velocity, and discharge under different flow conditions (up to several hundred measurements per station); (2) maximum annual peak discharges for at least 15 years of unregulated record for 72 of the stations; (3) time series of at least 10 years of unregulated daily discharges for 70 of the stations (out of the 72 stations with unregulated annual peak flows), and (4) time series of at least 5 years of unregulated hourly discharges

for 33 of the stations (out of the 70 stations with daily discharges).

2.2. Data Set II

[11] Data from the Neosho and Osage River basins in Kansas and Missouri, United States (see Figure 2), consist of (a) digital elevation models (DEMs) of the two basins at resolution 30×30 m, (2) lithologic logs of 420 water wells located within the floodplain boundary of channels with different contributing areas, and (3) high-resolution hydrography data (U.S. Geological Survey National Hydrography Data Set (NHDS)) for the two basins. The hydrography data are available in a vector format (polylines consisting of sequences of [X, Y] pairs) allowing representation of curvatures with radius of order $O(1-10$ m), which is impossible to derive from elevation raster data.

2.3. Data Set III

[12] Data from 114 stations in Nebraska, Iowa, Kansas, Missouri, and Oklahoma (see Figure 3) consist of independent measurements of suspended sediment load and suspended sediment concentration under different flow
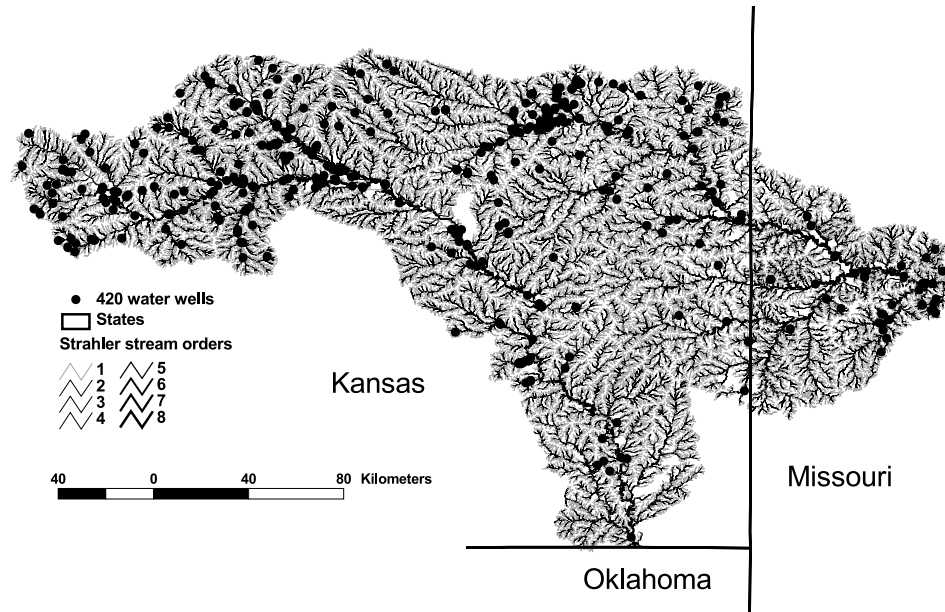
Figure 2. Map of Osage (East) and Neosho (West) River basins with the locations of the 420 water wells (data set II).

conditions (up to several hundred measurements per station).

3. Effect of Channel Morphometry on the Statistics of Daily Discharges and Extreme Floods

3.1. Determination of Bank-Full Channel Morphometry

[13] The determination of bank-full discharge and bank-full channel cross-sectional geometry is a difficult and tricky task and requires special attention. When field measurements of a channel cross-section are available, several geomorphic criteria for determining bank-full stage are usually applied [e.g., see *Williams*, 1978; *Richards*, 1982; *McCandless*, 2003]: (1) floodplain break, a discrete transition from near vertical to near horizontal cross-sectional profile; (2) scour line, a wear mark on a vertical bank, or a discrete break in the slope of the channel bank, distinguished from an inflection point by being farther down from the top of the bank; (3) depositional bench (natural levees), the flat surface, or highest elevation, of a lateral depositional surface other than a point bar; and (4) break above a point bar, the transition point from an inclining point bar surface to an horizontal floodplain surface (see Figure 4 for typical cross sections with definitions of the above terms). When measurements of discharge, stage, top width, and mean depth are available at a given gauging station for many different flow conditions, bank-full stage is considered to occur when a break in slope is observed in both stage-discharge and width-discharge relationships [e.g., see *Knighton*, 1984; *Leopold*, 1994, and references therein].

[14] Considering the high variability of cross-sectional shapes along a river reach, the determination of bank-full stage from field measurements is often a quite subjective task, including even the choice of a cross section to be surveyed. (A typical example could be a sharp transition from active channel to slowly inclining point bar with a weak transition to a floodplain, where the edge of the active channel can be considered as a floodplain break.) Furthermore, even if a river reach is properly surveyed at many cross sections, the averaged bank-full geometry and evaluated bank-full discharge can still significantly differ from the ones based on stage-discharge and width-discharge relationships. Figure 5 shows an example of bank-full channel geometry and bank-full discharge estimated from stage-discharge and width-discharge plots versus the ones estimated from a field cross-sectional survey at the same station [*Dutnell*, 2000]. This discrepancy is probably due to the fact that the behavior of a channel with geometry measured at a given cross section is not necessarily equivalent to the average flow through the reach, accounting for all the variability of channel shapes upstream and the nonlinear nature of flow hydraulics. This consideration is even more important for our analysis, as we are particularly interested in the determination of bank-full properties continuously over a large range of scales.

[15] For channels draining small contributing areas (of the order 100 km^2 or less) the determination of bank-full properties based on stage-discharge and width-discharge relationships is sometimes quite unreliable due to the fact that the floodplain might not be present at all and, consequently, the break in these relationships may not exist. This is why, for small contributing areas, bank-full geometry derived from field observations was added to increase the reliability of our analysis [*Dutnell*, 2000; *National Water Management Center*, 2004]. The plots in Figure 6 were created based on the bank-full properties estimated for 99 stations draining upstream contributing areas ranging from 2 to 65,000 km^2 (data set I). It is noted that the bank-full width W_{bf}, bank-full mean depth D_{bf}, and bank-full discharge Q_{bf} are directly estimated from the observations (and fitted by the solid lines on the plots of Figure 6), while the mean velocity at bank-full V_{bf}, cross-sectional area at bank-full C_{Abf} and the ratio D_{bf}/W_{bf} are derived properties
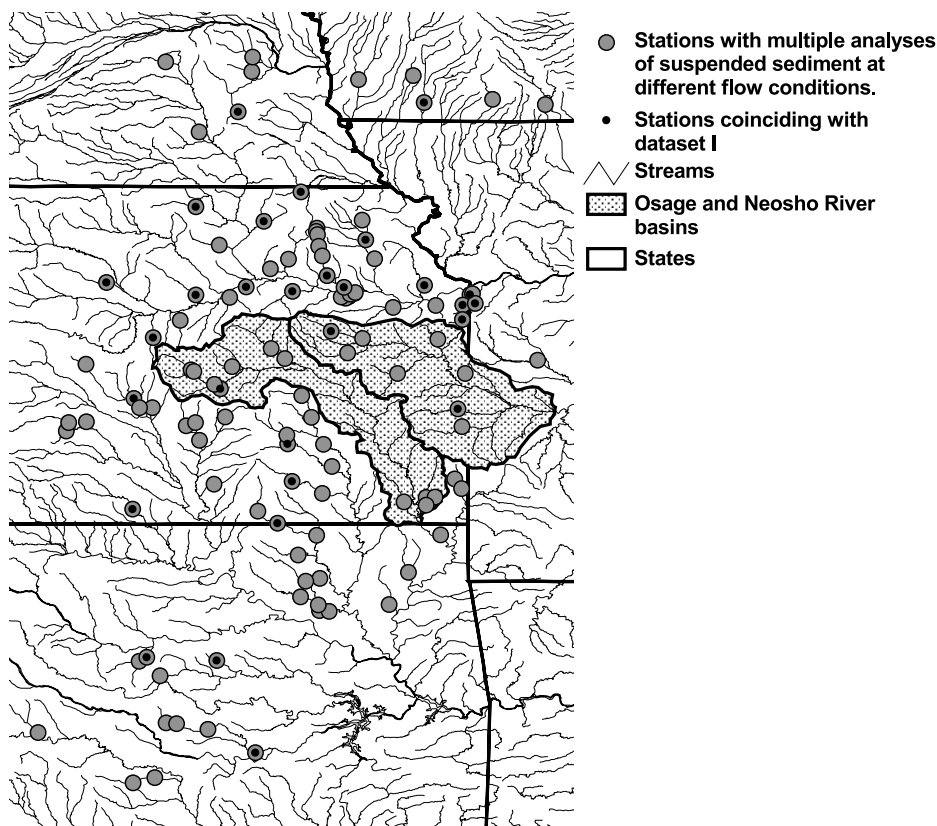
Figure 3. Locations of the stations with multiple samples of suspended sediment (data set III).

(and the broken lines in Figure 6 are derived from the fitted solid lines).

3.2. Channel Morphometry and Streamflow Statistics at a Cross Section

[16] To explore the effect of channel cross-sectional shape on streamflow statistics, we performed a parallel analysis of cross-sectional shape and probability distributions of daily discharges and maximum annual floods for data set I. A "characteristic cross section" was built for every station based on the half top-width versus stage relationship. (Note that this cross section is a symmetric version of the true cross section which is not available.) Figure 7 shows these characteristic cross sections together with the lognormal plots of daily and maximum annual discharges for three stations draining areas of approximately 400, 2000, and 13,000 km^2. The daily streamflow of probability of exceedance 80% (low flows), 20% (moderate flows), and the bank-full flows Q_{bf} have been positioned both on the frequency plots and on the channel cross sections. The purpose of this parallel analysis is to demonstrate that the statistics of both daily discharges and maximum annual floods are actually controlled by the channel shape. (It is noted that steeper slopes in the lognormal exceedance probability plot means lesser variability and thus thinner tails of the distribution, while the opposite is true for less steep slopes.) More specifically, in those parts of the channel cross sections where transverse slopes are relatively high above the active channel stage (more pronounced in cross sections in Figures 7b and 7c between $Q_{20\%}$ and Q_{bf}), the slope of the exceedance probability plots shows a tendency to decrease. This implies that the

variability of discharge increases, thus forming a "heavy" or "thick" tailed part of the distributions of daily discharges. In contrast, in the part of the cross sections with relatively low transversal slopes (and essentially for flows
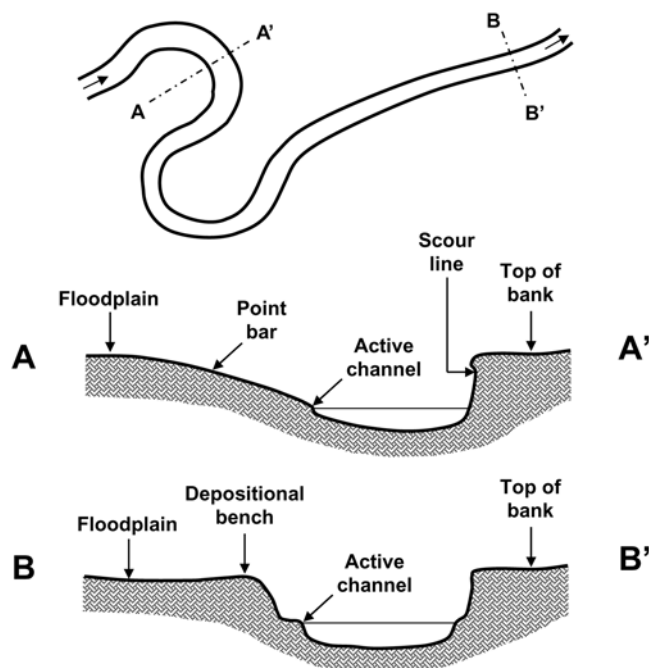

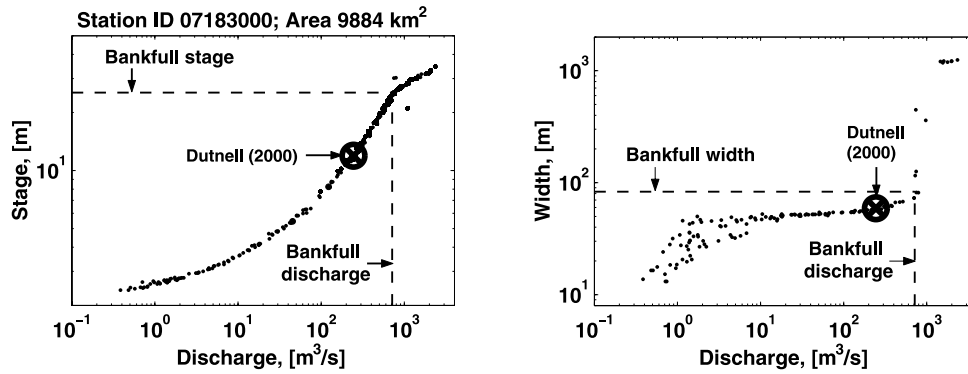**Figure 4.** Schematic of typical cross sections of meandering and straight channels.

Figure 5. An example of determination of bank-full discharge and bank-full width from stage-discharge and width-discharge plots compared with the corresponding values determined from a field survey.

slightly above bank-full) the slopes of the frequency of exceedance plots in both daily and maximum annual floods become steeper, implying that the variability reduces significantly at those streamflow ranges and thus forcing the tails of the distributions to become thinner within those ranges of discharge.

[17] Visual inspection of all flow duration curves and distributions of maximum annual floods one by one for all the 99 stations of data set I revealed the following overall behavior:

[18] In regime I, flow in the active channel approximately follows a straight line in a lognormal frequency plot (i.e., lognormal distribution) up to approximately the 20% quantile of exceedance.

[19] In regime II, in-channel flow up to bank-full shows increasing variability, forming a decreasing slope in the

frequency of exceedance curves or a heavily tailed part of the PDFs of daily and maximum annual flood discharges. This type of behavior is less pronounced in the downstream direction, where due to the increase of channel planform instability associated with channel migration and thus sinuosity [e.g., see *Dodov and Foufoula-Georgiou*, 2004b], flows over vegetated point bars become more and more frequent, introducing retardation effects and decreasing the variability of streamflow.

[20] In regime III, overbank flow with reduced variability forms a steeper slope in the frequency of exceedance curves or a thin tailed part in the PDFs of the daily and maximum annual flows.

[21] The three regimes are present in almost all flow-duration curves, although the individual shapes differ significantly from each other, which could be expected
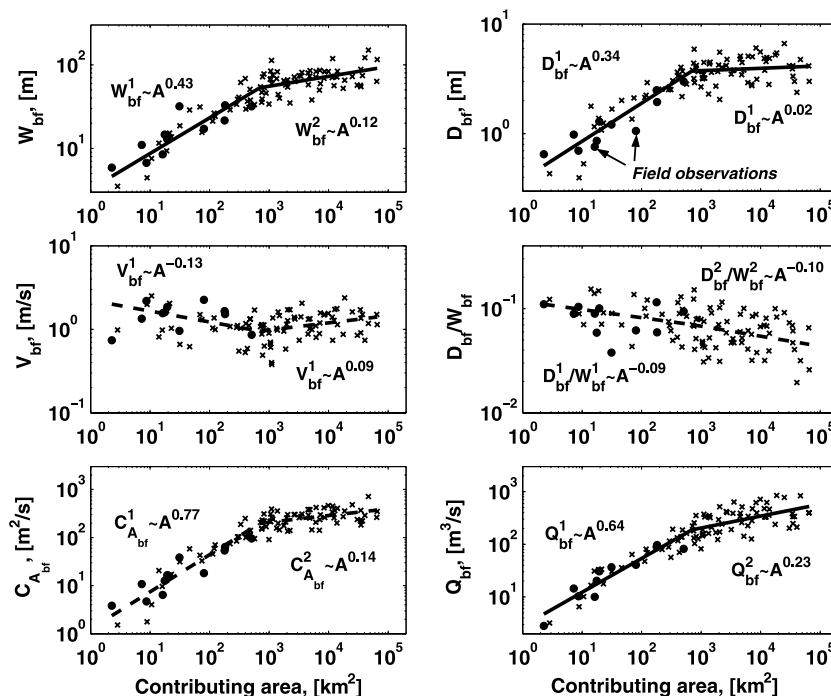

Figure 6. Dependence of the parameters of bank-full morphometry on scale (contributing area). Crosses represent bank-full parameters derived from the stage-discharge, width-discharge, and depth-discharge plots of data set I, and circles represent determination of bank-full properties based on field surveys. Solid lines are fitted by least squares, and broken lines are derived relationships from the solid lines.
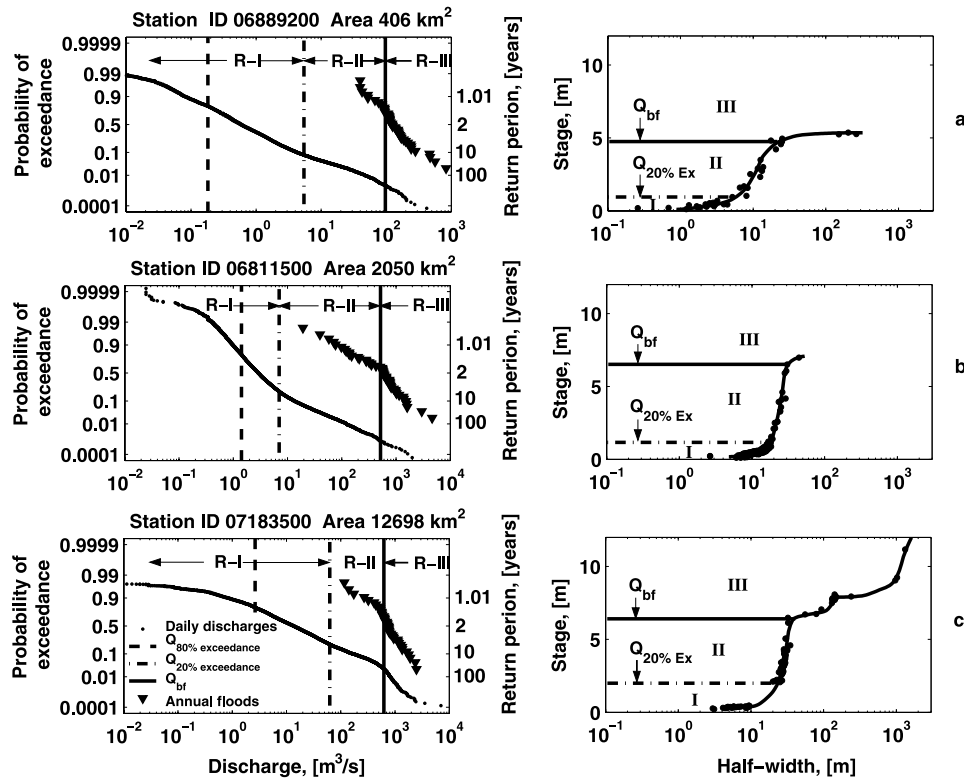
Figure 7. Lognormal plots of daily discharges and maximum annual floods for three stations together with the corresponding "characteristic" channel cross sections (built from the observed top-width versus stage relationships). Note that major changes in channel cross-sectional geometry correspond to major changes in the normal plots of both daily and maximum annual discharges suggesting strong dependence between channel cross-sectional shape and streamflow variability.

considering the enormous variability of cross-sectional shapes and the extent of the area under consideration. This type of behavior is so evident (especially for maximum annual discharges) that for many stations the break in the lognormal plot can be used for the determination of bank-full stage or other major changes in channel cross-sectional shape.

[22] Another important observation that can be made from the plots of Figure 7 is that the bank-full discharge seems to correspond to different frequencies of exceedance for channels draining small and large areas. A reasonable question arises then as to whether the frequency of exceedance of overbank flows is independent of contributing area (a common assumption in geomorphology [e.g., see *Leopold*, 1994, p. 134]) or whether it varies systematically with scale. Considering the effect that overbank flow has on the variability of discharge as documented above, it is obvious that this question is closely related to the scaling in floods and, in general, to how the statistics of streamflow change with scale.

3.3. Scale-Dependent Frequency of Bank-Full Discharge

[23] To test whether the transition to overbank flow occurs with different frequency for channels draining different contributing areas, in Figure 8 we plot the frequency of exceedance of Q_{bf} based on daily discharges versus scale (contributing area). Obviously, bank-full discharges are exceeded much more frequently for large scales than for

small ones. However, in the above analysis one should consider the fact that for very small catchments (for which response time is on the average shorter than 1 day) the temporal aggregation from instantaneous to daily mean discharges may significantly affect the flow-duration curve, thus generating a spurious upper tail of the distribution that is significantly thinner than the true one. Thus, for a fixed bank-full discharge (calculated by means of
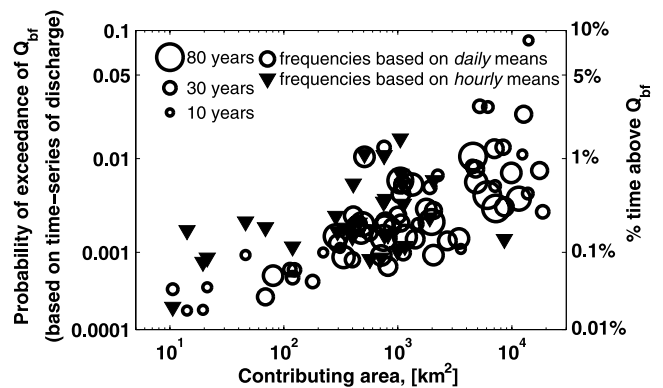

Figure 8. Frequency of exceedance of Q_{bf} as a function of scale based on daily and hourly time series. Note the increase in the separation between the two estimates for stations with contributing area less than approximately 500 km².
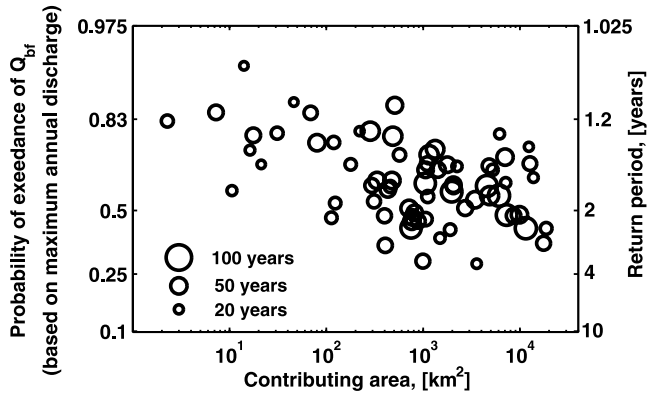
Figure 9. Frequency of exceedance of Q_{bf} as a function of scale based on maximum annual flood series.

practically instantaneous field measurements) at a station with contributing area of $O(10 \text{ km}^2)$, the calculation of its frequency of exceedance based on daily mean discharges may produce unrealistically low estimates, which is probably the case in Figure 8.

[24] To quantify the degree of this underestimation, we also plot in Figure 8 the probability of exceedance of Q_{bf} based on the available hourly time series of discharge. The comparison between the estimates based on daily and hourly discharges clearly shows that for streams with contributing areas less than 100 km^2 the underestimation is considerable, whereas this is not the case for streams draining larger areas. On the basis of this analysis, it is clear that the frequency of exceedance of bank-full discharge is not constant. For the area under investigation, channels draining small areas stay overbank approximately 0.1% of the time (on the average 1 day every 2–3 years) while streams draining large areas stay overbank approximately 1–2% of the time (on the average a week every year).

[25] The frequency of exceedance of bank-full discharge is often reported in terms of return period, i.e., based on maximum annual discharge frequency analysis. It is typically assumed that Q_{bf} has a constant return period of 1.5–2 years [e.g., *Chorley et al.*, 1984, chapter 7; *Leopold*, 1994]. As can be seen from Figure 9, which plots the probability of exceedance of Q_{bf} based on frequency analysis of maximum annual series, this is not the case for all contributing areas. Specifically, our analysis shows that for drainage areas of order $O(10^3)$ km^2 or larger, Q_{bf} has a return period of approximately 2 years (although it varies considerably between 1.2 and 4 years but with no apparent trend with scale) while for channels draining smaller areas this return period is much lower, i.e., approximately 1.2 years on average and ranging between 1.05 and 1.5 years, and shows a trend with scale. Considering the two frequency plots (Figures 8 and 9) together, it is apparent that channels draining larger areas go overbank less often (in terms of average number of occurrences per year) but stay overbank much longer (in terms of average number of days per year) than channels that drain smaller areas.

[26] Another interesting observation to make from Figure 9 is that for "larger" areas almost half of the maximum annual floods come from below and half from above bank-full flows, while for "smaller" areas the contribution of overbank flows to the maximum annual flow

series is much less and varies significantly with scale. The fact that overbank flows contribute in a scale-dependent way to the composition of maximum annual floods is expected to have significant consequences in the frequency analysis of maximum annual floods. This was already shown in Figure 7 where for flows above bank-full, a steeper slope in the lognormal probability of exceedance plots for maximum annual floods was observed, documenting that these floods (coming from overbank flows) have a decreased variability due to the "smoothing" effect of the floodplain.

4. Scaling of Daily Discharges and Floods Revisited: The Effect of Transition to Overbank Flows

4.1. The Need to Revisit Statistical Scaling Theories of Floods

[27] In this section we explore the effect of the scale-dependent transition to overbank flow on the scaling of daily discharges and maximum annual floods. From the breaks in the scaling of bank-full properties, inferred from the plots in (Figure 6) to be at a scale of around 700 km^2, and the connection of those properties to the different variability regimes for below and above bank-full flows (Figure 7), it is anticipated that the statistical moments of daily streamflow and maximum annual floods will exhibit a scaling break at approximately that same scale of 700 km^2.

[28] In Figures 10a and 10d we plot the first four moments of daily discharges and maximum annual floods as a function of contributing area. A break in scaling seems apparent (especially for the higher-order moments) at a scale between 500 and 1000 km^2. Assuming that the scale of the break is the same as that inferred previously from the scaling of the bank-full properties (which was around 700 km^2), we fitted straight lines to the log-log plots of moments versus area for the before and after the scaling break regimes. The plots of Figures 10b and 10e show the median slopes of these lines and the 5%, 25%, 75% and 95% confidence levels versus order of moment (the quantiles were computed under the assumption of lognormal error model and using a standard procedure for confidence interval estimation [e.g., see *Devore and Peck*, 1996]). It is clear that the slopes of the lines are significantly different for areas smaller and larger than 700 km^2, confirming thus the inference of a scaling break.

[29] Figures 10c and 10f display the CV of daily discharges and maximum annual floods versus scale. As expected, the scaling break is also reflected on the CV plots where one observes an almost constant (or slightly increasing) variability with scale up to approximately 700 km^2 and a decrease beyond. The differences in the slopes of the fitted lines are statistically significant for areas smaller and larger than 700 km^2. Considering the of log-log linearity of moments with scale in Figures 10a and 10d (a primary indicator for statistical scaling) and inferring a nonlinear behavior of the slope change with the moment order, one could assume existence of two multiscaling models, one with increasing variability up to 700 km^2 and another with decreasing variability for larger scales, for both daily discharges and maximum annual floods. We have not pursued the fitting of these multiscaling models although this is easy to do based on least squares fitting of the quantiles [see, e.g.,
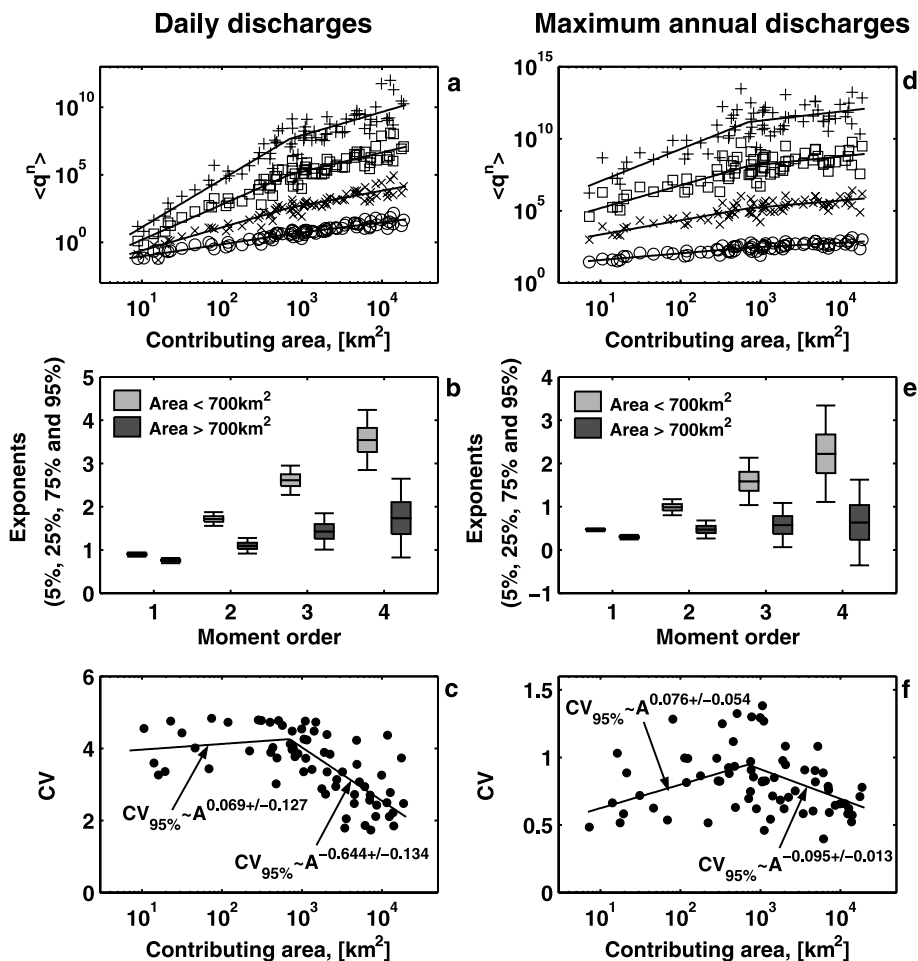
Figure 10. Log-log plots of the first four moments of daily and maximum annual discharges versus contributing area and fitted slopes of these lines for (top) contributing areas below and above 700 km^2, (middle) the confidence intervals of the slopes, and (bottom) CV versus contributing areas with fitted slopes.

Gupta et al., 1994; *Dodov and Foufoula-Georgiou*, 2004a]. Instead, as elaborated below, we critically question the applicability of the notion of statistical multiscaling to streamflow (daily discharges and maximum annual floods) in view of what we have established in the previous sections: (1) connections between channel morphometry and streamflow variability, and (2) transition to overbank flow with a probability which depends on scale.

[30] As discussed earlier, one can clearly see from Figure 9 that maximum annual floods come from two different populations (below bank-full and above bank-full discharges), and that the contribution of each of these populations strongly depends on scale. For example, for large areas almost half of the maximum annual flows come from above bank-full flows while for small areas only 15% do. This argument alone precludes one from approaching the problem of scaling in floods under the typical statistical multiscaling framework: The upper quantiles of the PDFs, which are dominated by overbank flows, change with scale in a specific physically imposed way which is different and nonconsistent with the way the lower quantiles change. This behavior precludes the existence of single normalization kernels $G(\lambda)$ (each within the different scaling regions) which can consistently "stretch" the PDFs over all scales and frequencies. It is interesting to note that the sensitivity

of scaling/multiscaling inferences to extremes (i.e., the tails of the maximum annual flood PDFs) has been reported before by *Pandey* [1998]. He used standard statistical moments and probability weighted moments (PWM) which are less sensitive to extreme values in the sample, and found that inferences about multiscaling differed depending on the technique: Simple scaling was inferred from the PWMs and multiscaling was inferred from the standard moments. This is not surprising based on our results which indicate that indeed the extreme values come from a different population altogether and as such the framework of statistical scaling for maximum annual floods must be used with caution and warrants more thorough examination in the future.

[31] For daily discharges, similar arguments apply. The flow duration curves are also affected (albeit to a lesser degree) by the morphometry of the channel and overbank flows (see Figure 7) which come into the picture with different frequencies at different scales (see Figure 8), and thus the notion of statistical scaling applied to daily discharges over all ranges of frequencies of exceedance must be seen again with caution. Nevertheless, if one looks at the moments of the daily discharges and the coefficient of variation (see Figure 10), a multiscaling model would be inferred. Such a model could provide a decent approximation, even if not grounded on solid theoretical-physical
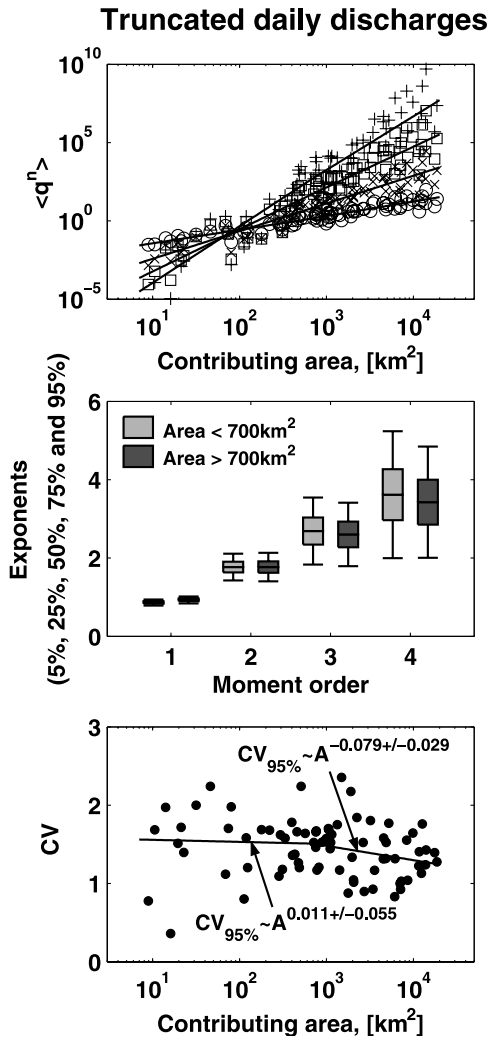
Figure 11. Same as Figure 10 but for daily discharges with truncated values corresponding to frequency of exceedance less than 5%.

computed using the Weibull plotting position) of daily discharge as a function of scale. It is observed that the low quantiles (exceedance frequency greater than 2.5%) are well approximated with single log-log linear relationships over all scales, while the high quantiles (exceedance frequency of the order of 0.05%) exhibit a break in scaling. For comparison, the bank-full discharge as a function of scale has been plotted in the same figure (taken directly from Figure 6). It is clear that as scale changes from small to larger, the 0.05% exceedance quantile of daily discharges is below (for small areas) and above (for large areas) the bank-full discharge. This demonstrates in a quantitative way that the break arises because of these scale-dependent contributions of overbank flows and that the scaling regime (heuristically characterized by how the slopes of the log-quantiles curves versus area change with the quantile level) changes in drastically different ways for small and large areas.

4.2. Physical Interpretation of Discharge Scaling

[33] To further understand Figure 12, let us try to explain it from a physical point of view, considering the "continuum" of frequencies of occurrence of different discharges:

[34] 1. When the flow is in regime I (see section 3.2 and Figure 7) the active channel is capable of conveying the supplied water and sediment without significant losses. This means that the discharges for any quantile above approximately 20% exceedance will be proportional to the contributing area drained by the channel (i.e., a straight log-log line with slope approximately 1). In this sense the flows in regime I can be considered as obeying a single simple scaling model.

[35] 2. In regime II the flow is still in the main channel but some retardation effects start taking place such as flow over point bars and through heavily vegetated banks. The effect of this type of behavior gradually increases downstream as the channel instability increases [see *Dodov and Foufoula-Georgiou*, 2004b], forcing the rivers to meander more and thus the flow to go more frequently over point bars. The effect of this type of behavior on the log-quantiles
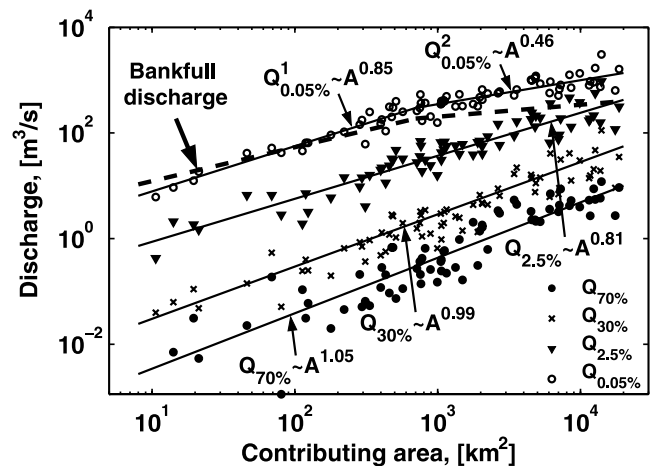
grounds for the reasons explained above. It is interesting to note that in our previous work [*Dodov and Foufoula-Georgiou*, 2004a] we employed a multiscaling model (which ended up being close to a simple scaling model after estimation of parameters) for daily discharges and used it to derive generalized hydraulic geometry (HG) relationships. It is emphasized that the daily discharges that were relevant to these HG relationships are the below bank-full discharges and as such their approximation with a multiscaling model is not in error. To confirm this more quantitatively, it is noted that if one excluded from the estimation of moments the very high quantiles of exceedance, by truncating the PDFs of daily discharges to below 5% probability of exceedance (necessary to neglect the effect of overbank flows according to Figure 8), and performed a moment analysis, then the moments and CV of Figure 11 would be observed, indicating that in fact, a single multiscaling model would not be an unreasonable approximation for below bank-full discharges over the whole range of scales. This issue needs more careful examination on its own right.

[32] Figure 12 shows several empirical quantiles (frequencies of exceedance of 70%, 30%, 2.5%, and 0.05%

Figure 12. Plot of the empirical quantiles of daily discharges with frequencies of exceedance 70%, 30%, 2.5%, and 0.05% as a function of scale. The approximated trend from Figure 6 for bank-full discharges is also plotted for comparison.
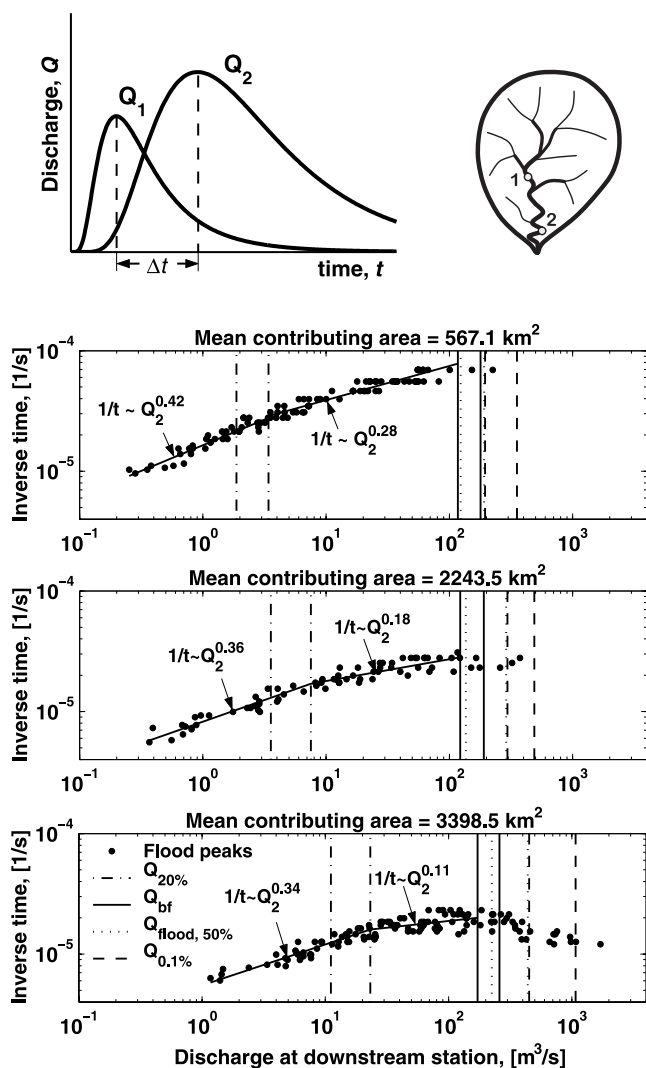
Figure 13. Analysis of the effect of channel morphometry on flood wave celerity. The daily discharge quantiles of exceedance $Q_{20\%}$, $Q_{0.1\%}$, the bank-full discharge Q_{bf}, and the median of the maximum annual discharges $Q_{flood,50\%}$ are given for both the upstream and downstream stations.

versus log-scale plots is that such plots can still be approximated by straight lines, but with slopes less than 1 (i.e., the relation between discharge quantile and contributing area becomes nonlinear with exponent less than 1, thus accounting for the gradual increase of this effect in the downstream direction). Since the slopes will diverge from 1 faster when the flow approaches bank-full discharges (i.e., the higher the discharge the higher the resistance to flow over point bars with an increase of this effect in the downstream direction), a single multiscaling model can be used as a working model to describe the flow in this regime (see *Dodov and Foufoula-Georgiou* [2004a] for details).

[36] 3. In regime III the variability of discharges rapidly decreases due to occurrence of overbank flows, forcing the log-quantiles versus log-scale plots to become nonlinear with a break at ∼700 km² where the break in log-bank-full geometry versus log-scale occurs (see Figure 6).

[37] A direct consequence of the above considerations is that the propagation of a flood wave through a river network

should be strongly affected by the transition to overbank flow, with an emphasis on the scale-dependence of this process. In the next section we provide an independent test for the ideas outlined above by analyzing flood wave celerity as a function of both flow conditions and scale.

4.3. Flood Wave Propagation Analysis: The Effect of Scale-Dependent Transition to Overbank Flows on Streamflow Dynamics

[38] On the basis of 5 years of hourly streamflow observations for three pairs of stations, one upstream and the other downstream (see Figure 1), we were able to calculate the time necessary for a flood wave to propagate between the two stations. In Figure 13 we plot the inverse of this time versus the peak hydrograph discharge of the downstream station for many flood events of different magnitudes for every one of the three pairs of stations (corresponding to mean contributing areas of 567, 2243, and 3398 km², respectively). It is noted that the inverse time is equivalent to wave celerity without, however, considering the distance between the stations which, especially for meandering rivers, depends on the scale of the source map. On the graphs of Figure 13, the bank-full discharges, the median annual flood discharges, and the discharges corresponding to 20% and 0.1% probability of exceedance (based on mean hourly flows) are plotted. Two facts supporting our previous discussion on the scale-dependence of hydrologic response become obvious from these plots: (1) The rate of increase of wave celerity with discharge below the 20% quantile (regime I) is almost the same for the three stations (i.e., similar slopes); (2) with an increase of discharge in regime II the slope decreases faster for larger contributing areas, which implies more resistance to flow in the downstream direction, and (3) in regime III, with an increase in contributing area, the separation between the bank-full discharge and the median annual flood and the 0.1% quantile of hourly discharges becomes more and more evident, and consequently, a larger and larger part of the river reach goes overbank, and as a result significant retardation effects take place and affect wave celerity.

[39] The above example provides one more piece of evidence in support of the ideas outlined in the previous section, namely, that the systematic variation of channel morphometry downstream, and respectively the scale-dependent transition to overbank flow, are important factors affecting in a different way both streamflow statistics and streamflow dynamics as the contributing area increases. Up to this point, however, we considered only how this effect takes place. The question of why the transition to overbank flows depends on scale (i.e., what is the physical reason for this transition) is the subject of the next section.

5. Covariation of Scaling Regimes and Scaling Breaks in the Coupled Hydrogeomorphologic System

5.1. Scaling of Bank-Full Morphometry and Streamflow Variability

[40] In section 3 we considered the effect of channel morphometry on streamflow variability as a function of scale. Here we pose the question as to whether there is a feedback from streamflow variability (and how it varies
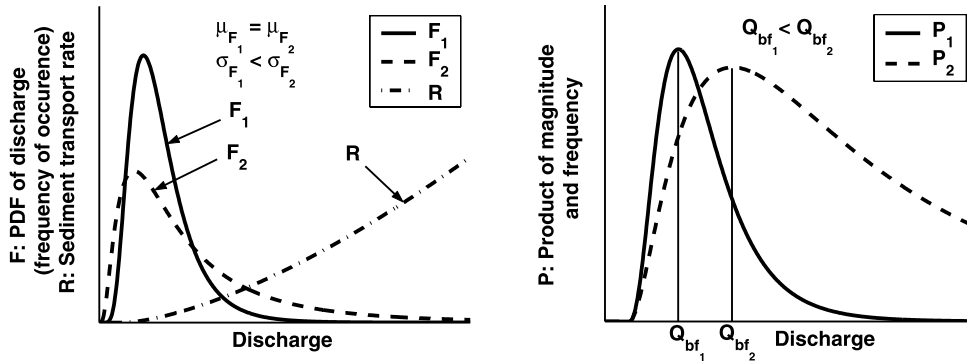
Figure 14. Example of the effect of variability of formative discharge on the magnitude of the equivalent dominant discharge.

with scale) to the channel bank-full morphometry (and its variation with scale). For this, we employ the concept of "equivalent dominant discharge" (EDD) introduced by *Wolman and Miller* [1960]. The equivalent dominant discharge is assumed to be the discharge that performs the most work (the work being defined in terms of sediment transport) and is determined as the discharge at which the maximum of the product between the frequency of occurrence (PDF of discharge) and the sediment transport rate curve (sediment load L_s versus water discharge Q_w) occurs (see Figure 14). The concept of dominant discharge acknowledges the fact that frequency as well as magnitude of flows determine their geomorphic effectiveness, measured in terms of the relative quantities of sediment transported, and thus their potential for modification of the surface form and channel shape. The problem of relating the dominant discharge (in terms of magnitude and frequency) to the variability of flows and the size of the drainage basin was attempted early on via physical arguments and limited empirical analysis. For example, *Wolman and Miller* [1960,

p. 58] commented that "the greater the variability of runoff, the greater the % of the total load which is carried by infrequent flows." They also argued and confirmed empirically that "because runoff becomes increasingly variable as drainage area A is reduced, the smaller the A the larger % of sediment will be carried by less frequent flows." These statements have the potential to be quantified in more specific terms, since we have established how the discharge variability changes with scale. This is attempted below.

[41] To demonstrate the effect of discharge variability on the magnitude of the dominant discharge at a given cross section, we consider in Figure 14 an example with two lognormal distributions with equal means but different standard deviations (i.e., different CVs) while the sediment rate curve is assumed to be the same for both cases. Clearly, the product of the sediment rate curve with the PDF of larger CV results in a larger dominant discharge and respectively larger channel morphometric parameters and conveyance. Now, if we consider that the CV of discharges changes with scale as shown in the bottom panels of
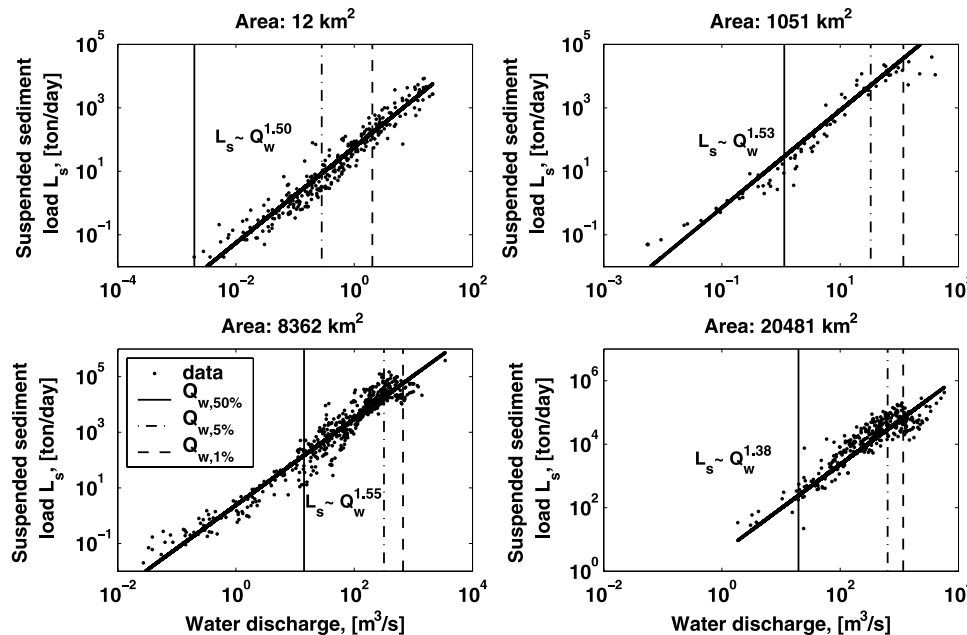

Figure 15. Suspended sediment load (L_s) versus water discharge (Q_w) plotted for several stations of different contributing areas.
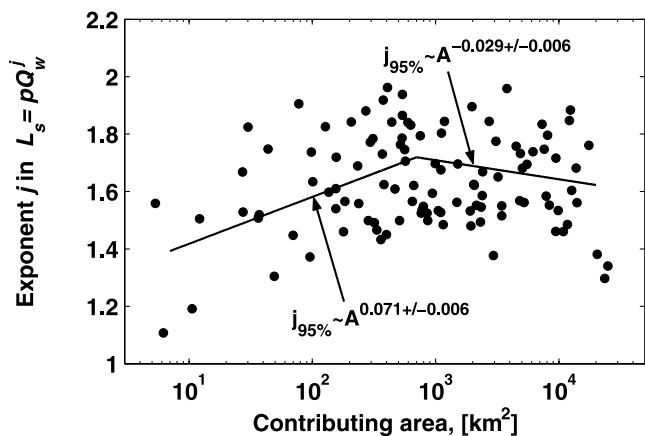
Figure 16. Exponents of the power law approximations of at-station L_s versus Q_w relationships as a function of scale.

Figure 10, i.e., increasing CV up to a scale of approximately 700 km² and decreasing CV afterward, it is expected that the same trends with scale will show up in the dominant discharge, and also in the channel bank-full properties with scale. Such a behavior is evident from Figure 6 for channel morphometric properties and for Q_{bf} (often equated to the dominant discharge [e.g., see *Wolman and Miller*, 1960; *Andrews*, 1980]). This establishes not only the fact that channel morphometry affects the statistics of discharges (as shown in section 3) but also that both the magnitude and the variability of discharge affect in turn the channel morphometry.

[42] The most important consequence of the above discussion is that streamflow statistics and channel cross-sectional geometry are mutually dependent, with a dependence that has its own specifics at each given site, but changes in a consistent way across a large range of scales. Furthermore, this dependence is expected to manifest itself in two other physical attributes of the fluvial system: (1) suspended sediment supply and how it changes with scale, and (2) floodplain development and how it changes with scale. These two aspects are analyzed in the next sections.

5.2. Scaling of Suspended Sediment Rate

[43] The scale-dependent transition to overbank flow documented in Figures 8 and 9 is expected to show its effect on the suspended sediment carried by the system for near-bank flows. To test this conjecture, we analyzed the data from the 114 stations of data set III. These data consist of enough (up to several hundred) observations of suspended sediment concentrations and water discharges at every station to allow the construction of sediment rate curves (suspended sediment load L_s versus water discharge Q_w in the log domain). Figure 15 shows several examples of such plots for four stations draining areas approximately 10, 1000, 8000, and 20,000 km². Although there is a considerable scatter, power law relationships of the form $L_s = pQ_w^j$ [e.g., see *Leopold and Maddock*, 1953] can be comfortably assumed for all stations. In Figure 16 we show the power law exponents j fitted to all available stations, plotted as a function of contributing area upstream from each station. Despite the considerable scatter of these exponents, one can observe an increasing tendency up to areas of approximately

1000 km² and a decreasing tendency of the exponents for larger areas. In fact, assuming that the previously inferred transition of channel morphometry and flow regimes at a scale of approximately 700 km² carries also to the suspended sediment transport rates, the linear trends fitted to the slopes j versus scale for areas below and above 700 km² show statistically significant differences (see Figure 16).

[44] In Figure 15 we have positioned several quantiles of daily discharges, i.e., quantiles of 50%, 5%, and 1% frequency of exceedance in order to consider two quantiles below bank-full and one quantile affected by overbank flows. Upon closer inspection of all sediment rate curves, it was concluded that power laws offer good approximations over the whole range of water discharges only for channels draining contributing areas approximately less than 100 km², while for streams draining larger areas the sediment load levels off or even slightly decreases below the 5% quantile of discharge. This type of behavior is more pronounced for contributing areas larger than approximately 1000 km² and becomes increasingly so as scale increases. Such a trend is better seen in Figure 17 where we plot the suspended sediment loads conditional on the above three quantiles of discharge as a function of scale. While the 50% and the 5% quantiles follow approximately straight parallel lines in log-log space, the 1% quantile follows quite a different trend. The slight change in slope around 700 km² in Figure 17 suggests that the rate of increase of the suspended sediment load does indeed decrease significantly during overbank flows, with the trend becoming more prominent with increasing scale.

[45] Scaling laws for suspended sediment load are important for ecologic and geomorphologic studies and to our knowledge have not been considered before. It is emphasized that the selected quantiles correspond to daily discharges of water Q_w and are not necessarily the same quantiles for sediment load L_s. The quantiles would coincide only in the case that Q_w and L_s are related via a power law, i.e., log-log linear, and the PDF of Q_w is lognormal. On the basis of our previous results this approximation would hold for the 50% quantile and partly for the 5% quantile but not for the 1% quantile of Q_w.
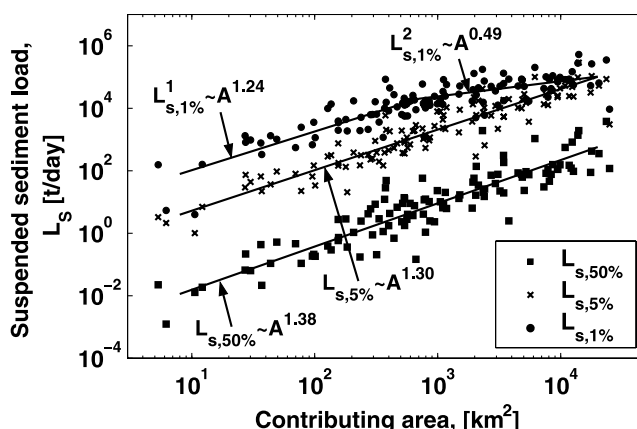

Figure 17. Suspended sediment loads (L_s) corresponding to three quantiles of water discharge (Q_w) (probability of exceedance 50%, 5%, and 1%, i.e., $Q_{w,50\%}$, $Q_{w,5\%}$, $Q_{w,1\%}$ as shown in Figure 15) as a function of scale.
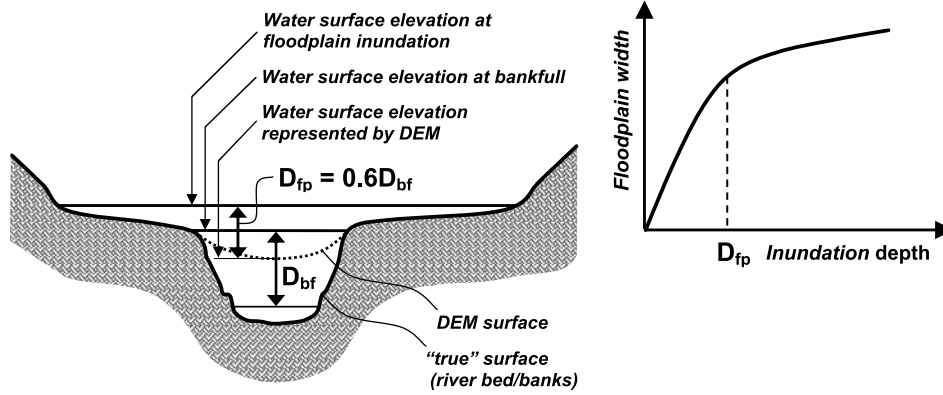
Figure 18. Illustration of the simple rule used for floodplain extraction from a digital elevation model (DEM).

[46] If the rate of increase of the suspended sediment load in the channel shows a decrease in the downstream direction as inferred from Figure 17, then it is reasonable to assume that this change might be due to increasing sediment loss associated with floodplain construction. It is noted, however, that the main process of floodplain generation is through meandering and lateral erosion under overall net preservation of sediment. Therefore, if our physical explanation of the connection between variability of streamflow and channel bank-full morphometry outlined in the previous section is correct, then in order to accommodate the additional sediment supply, the floodplain would be expected to increase not only in its width but also in its depositional depth. This issue is examined in the next section.

5.3. Scaling in Floodplain Morphometry

[47] To verify the conjecture that for drainage areas larger than approximately 700 km^2 the floodplain will start increasing its width and its depositional depth in the downstream direction, we performed a floodplain extraction algorithm based on the digital elevation model (DEM) of the Neosho and Osage River basins, Kansas (data set II). (Applying the same procedure for 30 × 30 m DEM grid over the whole region of interest would not be feasible.)

[48] The underlying assumption of the floodplain extraction algorithm is a simple rule of thumb: The depth of inundation used to define the lateral extent of the floodplain is proportional to the depth of the channel at bank-full flow. Although such an intuitive connection is in general accepted by geomorphologists (Gary Parker, Chris Paola, and Kelin Whipple, personal communication, 2004), to the best of our knowledge it has never been supported by a geomorphologic analysis. Such an analysis for the determination of the proportionality constant was introduced recently by *Dodov and Foufoula-Georgiou* [2005], and the results of this analysis are also used in the present work. The underlying procedure of the proportionality constant determination is based on the estimation of the floodplain width as a function of inundation depth for all channels representing a given scale (in terms of contributing area or Strahler stream order). The inundation depth above the river water surface elevation represented by the DEM at which this relationship has maximum curvature was assumed to correspond to the lateral extent of the floodplain. This assumption was made because with an increase of the inundation depth after this point, the above relationship levels off due to the increasing steepness of the valley transverse slope (see Figure 18 for an illustration and *Dodov and Foufoula-Georgiou* [2005] for technical details). The analysis conducted by *Dodov and*
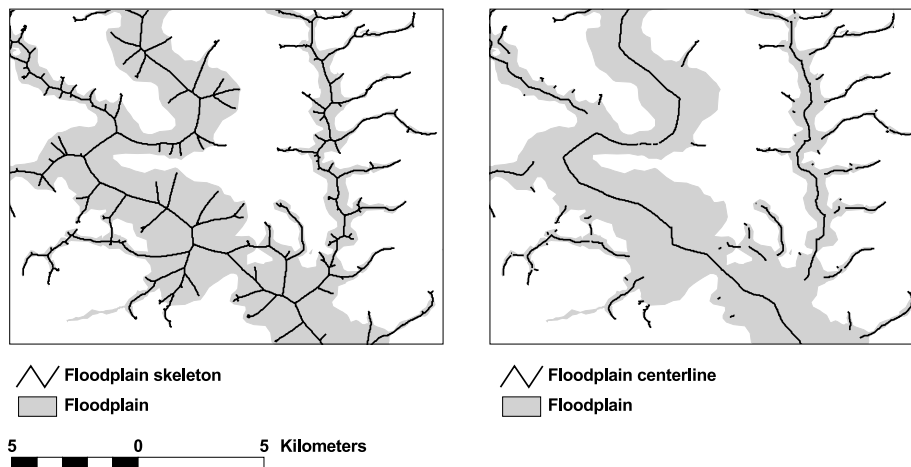

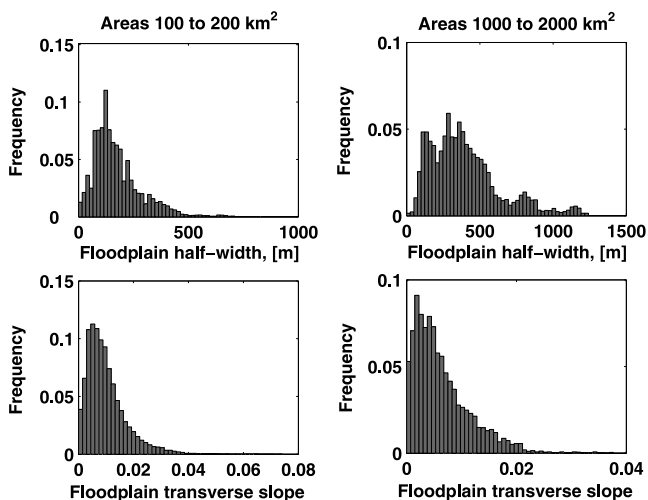**Figure 19.** Example of extraction of (left) floodplain ''skeleton'' and (right) floodplain centerline.

Figure 20. Probability distributions of floodplain half widths and transverse slopes for channels with contributing areas 100–200 and 1000–2000 km^2.

Foufoula-Georgiou [2005] showed that the floodplain inundation depth and bank-full depth at any given scale are linearly related with a coefficient of proportionality $p = 0.6$, i.e., $D_{fp} = 0.6D_{bf}$. This proportionality constant was also adopted in the present study.

[49] As documented in Figure 6, the channel depth at bank-full flow can be approximated as a power law of the contributing area with exponent 0.34 for areas less than 700 km^2 and almost constant (exponent of 0.02) for larger areas. These two power laws were used in the floodplain extraction procedure to compute the effective depth of floodplain inundation at any given scale. Then the decision as to whether a pixel belongs to the floodplain was made based on a local scale-dependent function, accounting for the curvature of the channel and the location of the point (see details given by *Dodov and Foufoula-Georgiou* [2005]). After the floodplain was extracted, its centerline was determined using the so-called "medial axis transform" procedure [e.g., see *Prasad*, 1997]. An example of floodplain skeleton and centerline extraction is shown in Figure 19. Since every pixel of the floodplain centerline can be assigned a contributing area, distance, and a direction to the floodplain boundary, we can perform a statistical analysis and plot the median floodplain half

width and median transverse slope as a function of scale (median because the distributions of the floodplain widths and transverse slopes are skewed as shown in Figure 20). Such a plot is given in Figure 21, suggesting that the floodplain width (transversal slope) starts to increase (decrease) faster above ~700 km^2, which is exactly what we would expect to see based on the previous discussion. It is interesting to also observe how the ratio of floodplain half width to channel half width changes as a function of area (see Figure 22). Up to areas of approximately 700 km^2 this ratio is almost constant, and for larger areas the growth of floodplain width relative to that of the channel goes as ~A$^{0.42}$.

[50] The last piece of our analyses is to check whether there is a significant change in the floodplain depositional depth versus contributing area at a scale around 700 km^2. To perform this analysis, we used the lithologic logs of over 400 water wells in Kansas and Missouri, located not farther than one river width from the river centerline (see Figure 3). The river width was approximated by the power laws of the width versus area plot in Figure 6. Bedrock was assumed to be shell or limestone according to the specific log, and the floodplain deposit was assumed to consist of unconsolidated clay, silt, sand, and/or gravel. In Figure 23 we plot the depth to bedrock as a function of scale (after assigning contributing area to every log). As can be seen from this figure, the depth of deposit to bedrock rapidly increases after ~600 km^2, clearly suggesting a transition from net-erosional (almost constant depositional depth of what is likely a poorly developed floodplain) to a well-developed net-depositional fluvial regime (discontinuity and rapid increase of floodplain depositional depth downstream).

5.4. A Physical Explanation of the Break and Different Scaling Regimes in Terms of the Connection Between Hydrologic and Geomorphologic Processes

[51] On the basis of analysis of stream cross-sectional geometry, daily and maximum annual discharges, suspended sediment load, and floodplain geometry as a function of scale, the following coherent picture emerges as a physical explanation of the observed covariation in scaling regimes and scaling breaks in the hydrology and fluvial geomorphology of these systems.

[52] 1. For contributing areas less than approximately 100 km^2, it is seen that rivers flood frequently (Figure 9) but remain overbank for only a small fraction of time (Figure 8). Both the frequency of flooding and the fraction
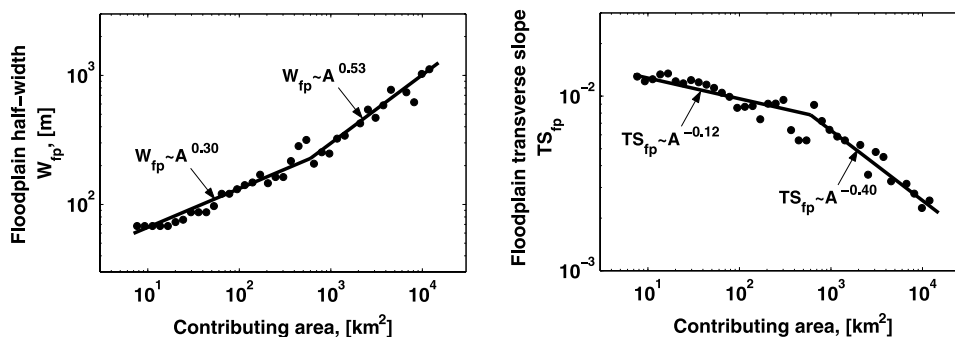

Figure 21. Plot of (left) median floodplain half width and (right) transverse slope versus contributing area.
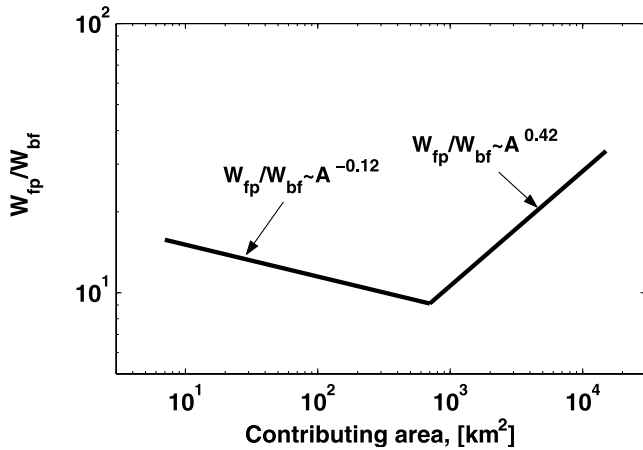
Figure 22. Plot of the ratio of floodplain width and channel width as a function of scale.

of time the flow is overbank vary little with contributing area within this range (the former increases weakly and the latter is approximately constant with contributing area). Since for streams draining areas less than 100 km^2 the floodplain is narrowest (Figure 21) and the depth of alluvium deposit is thinnest (Figure 23), it is reasonable to infer that such streams have relatively poorly developed floodplains constructed by frequent, short floods. The result from the frequent occupancy of floodplain by overbank flows is reflected by reduced variability of peak discharges (decreasing CV with decreasing scale in Figure 10f), which (according to the EDD concept) in turn suppresses the rapid increase in channel conveyance.

[53] 2. With an increase of contributing areas to ~700 km^2, rivers flood ever less frequently (Figure 8), but remain overbank for ever longer fractions of time (Figure 9). That is, the channel morphology is created by progressively rarer but longer floods. The increasing floodplain width (Figure 21) and depositional depth (Figure 23) suggest that the channels at this range of scales have relatively better developed floodplains, wide enough to support a higher channel sinuosity than streams with contributing areas less than 100 km^2. This favors the cross-sectional shapes illustrated in Figure 4a, where increasing flood discharge can spread out over the point bars of the meanders before it goes overbank. This difference in sinuosity and associated channel structure may be the reason that channel cross sections with contributing areas between 100 and 700 km^2 show a lower frequency of bank-full flow than those with smaller contributing areas (Figure 9). At the same time, the increased variability of channel sinuosity with scale [see *Dodov and Foufoula-Georgiou*, 2004b] increases the variability of flood peaks which achieves maximum at the scale of about ~700 km^2 (see Figure 10f). The increased variability of peak discharges in turn favors an increase of channel conveyance downstream according to the EDD concept (as can be seen from Figure 6).

[54] 3. Plots of many parameters show consistent breaks in trends as the contributing area increases above ~700 km^2. These breaks are apparent in five of the six plots of Figure 6 (for example, bank-full discharge, width, and depth all increase less rapidly with increasing contrib-

uting area beyond 700 km^2). Figure 21 shows that floodplain width increases more rapidly, and floodplain transverse slope decreases more rapidly with increasing contributing area beyond 700 km^2. Finally, a similar break is evident in Figure 23, indicating that the thickness of floodplain alluvium increases more rapidly with increasing contributing area beyond 700 km^2. It is argued here that these breaks in trends are likely due to a transition from an overall mildly erosional regime upstream, which suppresses floodplain development, to a more depositional regime downstream, which enhances floodplain development. Wider, deeper floodplains offer rivers the freedom to develop highly sinuous channels with well-developed point bars and the cross-sectional shape illustrated in Figure 4a. The well-developed floodplain together with the decreased rate of increase of channel conveyance (Figure 6) is reflected by overbank flows with slightly increasing frequency of occurrence (Figure 8) and even longer duration (Figure 9) acting as long-term temporal storages and thus significantly reducing variability of peak flows (Figure 10). According to the EDD concept the reduced variability of peak discharges is in turn reflected by a lower rate of increase of channel conveyance (Figure 6). The break in trends at the scale of approximately 700 km^2 illustrates the consequences of an interaction between stream hydrology and morphology that changes character with increasing scale. Although our explanation is well supported by extensive analysis of observations, a deeper understanding of the complicated relations between space-time rainfall and the specifics of fluvial processes at a given scale requires further analysis.

6. Summary and Conclusions

[55] This paper reports the results of an effort to understand and quantify the coupled hydrologic-geomorphologic system and relate the morphometry of channels and floodplains to the variability and scaling of floods and sediment loads across a range of scales and frequencies. The study is based on a comprehensive analysis of hydrologic and geomorphologic observations which include channel cross-sectional morphometry, daily discharges and maximum annual floods, suspended sediment loads, as well as high resolution hydrography, digital elevation models, and sed-
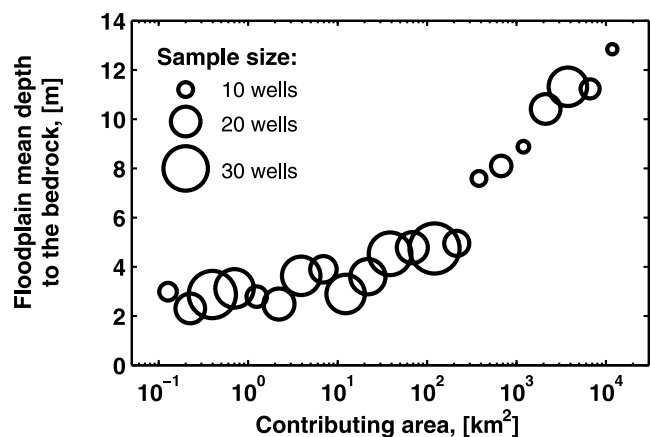

Figure 23. Plot of floodplain depositional depth versus contributing area.

imentary log data for extraction of floodplain morphometry. It builds on previous work by the authors which examined, based on statistical as well as physical grounds [*Dodov and Foufoula-Georgiou*, 2004a, 2004b], how and why the relationships between channel morphometry and discharge (known as hydraulic geometry, or HG) might change with scale and the effect this scale-dependency would exert on hydrologic response. The present study takes a closer look at the interaction of fluvial and hydrologic processes and poses some important hypotheses as to the origin and nature of these interactions as they manifest themselves over different scales and frequencies of discharge. Overall, a coherent picture emerges that supports a strong connection between the channel-floodplain interactions and their signature on the scaling regimes of the hydrologic and geomorphologic processes.

[56] The main results of this study are summarized as follows:

[57] 1. The channel cross-sectional geometry exerts a strong control on the shape of the flow duration curves and on the frequency distribution of maximum annual floods.

[58] 2. On the basis of the concept of dominant discharge, it was argued that the scale-dependent distribution of discharges dictates the way the equivalent dominant discharge (the discharge that performs most of the work in terms of sediment transport) changes with scale and thus affects the resulting channel morphometry.

[59] 3. It was demonstrated that the frequency of exceedance of the bank-full discharge is scale dependent and, in particular, that channels draining large areas flood less often (in terms of return period) but stay overbank much longer (in terms of days per year) than channels draining small areas.

[60] 4. It was shown that the critical area (scale) at which the variability of floods with scale changes from increasing to decreasing associates with the scale at which the fluvial regime changes from net-erosional to net-depositional and the floodplain becomes well established due to its increased frequency of occupation by the flow. An important practical implication of this finding is that it allows the determination of the critical area at which the scaling break in floods occurs based on a channel/floodplain morphometric analysis.

[61] 5. Scaling relationships of suspended sediment transport rates were computed and were shown to depend on the frequency of discharge. For streams draining large contributing areas, a significantly reduced rate of suspended sediment load per unit area emerges, as more frequent deposition of this sediment on the floodplain takes place.

[62] 6. It was argued that a maximum annual flood series is composed of two distinct populations, one from below bank-full flows and the other from above bank-full (floodplain) flows, and that the contribution of each population is scale dependent. As such, very extreme floods should not be seen as more intense and rarely observed versions of the more normal flows, but as the manifestation of a different population controlled by different dynamics. Under this argument, the current notion of statistical scaling in floods (even with a break in scaling at a certain scale) is physically questionable and must be applied with caution. The same argument applies to daily discharges, although to a lesser degree.

[63] The results of our study presented quantitative evidence for the impact of fluvial processes on streamflow statistics and dynamics, and the feedback these provide to the channel self-adjustment and to the floodplain. They also pointed out to a characteristic scale (in our study ∼700 km^2) at which some physical transitions occur leaving their imprint on the statistical scaling laws of hydrologic and geomorphologic variables. However, one open question still remains: Why does the transition from net-erosional to net-depositional fluvial regimes occur at the scale of ∼700 km^2 at least for the midwestern U.S. region? Our intuitive guess is that this scale (under uniform geologic conditions) may be related to the space-time intermittent nature of rainfall for that region, the river network topology, and the sediment supply regime. It is interesting to note that analysis of midlatitude convective storms over the Oklahoma/Kansas region [e.g., *Perica and Foufoula-Georgiou*, 1996] suggests that the spatial correlation length of these storms is of the order of 25–30 km, implying a spatial imprint of "coherent" rainfall features of the order of 700 km^2. That this scale coincides with the scale at which the geomorphologic signature of transition to floodplain formation was found needs to be further investigated. Incidentally, a similar analysis in the Appalachian highlands shows that in that region the scale at which the scaling break in floods occurs is approximately 100 km^2 (as also documented by *Smith* [1992] and *Gupta et al.* [1994]) and this scale coincides with the scale at which a scaling break is also found in the floodplain morphometry [see *Dodov and Foufoula-Georgiou*, 2005]. This provides further evidence for the intricate coupling between hydrologic and geomorphologic processes and its effect on the scaling of flows, channel and floodplain morphometry, and sediment transport. Further probing on this question, i.e., understanding the geomorphologic controls on hydrologic response and flood frequency statistics, needs to explicitly include the space-time variability of precipitation. This can be accomplished via distributed model simulations similar to the ones of *Menabde and Sivapalan* [2001], but accounting for the space-time intermittency of rainfall and the scale-dependent channel-floodplain interactions. Such simulations based on the methodology proposed by *Dodov and Foufoula-Georgiou* [2004c] are the subject of ongoing research.

[64] Another subject of future research relates to reconciling the current statistical scaling theories of floods with the geomorphological constraints arising from the channel-floodplain interactions. Such reconciliation can build either on the existing theoretical frameworks upgraded by the mixture model concept (such as the mixed bivariate lognormal multiscaling model introduced by *Dodov and Foufoula-Georgiou* [2004a]) or explore new statistical frameworks emerging in the context of scaling in mixed-physics phenomena (e.g., phase transition in multifractal scaling) [see *Arneodo et al.*, 1995, and references therein].

References

Andrews, E. D. (1980), Effective and bankfull discharges of streams in the Yampa River Basin, Colorado and Wyoming, *J. Hydrol.*, *46*, 311–330.

Arneodo, A., E. Bacry, and J. F. Muzy (1995), The thermodynamics of fractals revisited with wavelets, *Physica A*, *213*, 232–275.

Chorley, R. J., S. A. Schumm, and D. E. Sugden (1984), *Geomorphology*, Methuen, New York.

Dalrymple, T. (1960), Flood frequency methods, *U.S. Geol. Surv. Water Supply Pap.*, *1543-A*, 11–51.

Devore, J., and R. Peck (1996), *Statistics: The Exploration and Analysis of Data*, 3rd ed., 852 pp., Duxbury, Pacific Grove, Calif.

Dodov, B., and E. Foufoula-Georgiou (2004a), Generalized hydraulic geometry: Derivation based on a multiscaling formalism, *Water Resour. Res.*, *40*(6), W06302, doi:10.1029/2003WR002082.

Dodov, B., and E. Foufoula-Georgiou (2004b), Generalized hydraulic geometry: Insights based on fluvial instability analysis and a physical model, *Water Resour. Res.*, *40*(12), W12201, doi:10.1029/2004WR003196.

Dodov, B., and E. Foufoula-Georgiou (2004c), Representation of channel morphology and river network topology as a dynamic Bayesian network: Towards a probabilistic runoff routing, *Eos Trans. AGU*, *85*(17), Joint Assembly Suppl., Abstract H22B-05.

Dodov, B., and E. Foufoula-Georgiou (2005), Floodplain morphometry extraction from a high resolution digital elevation model: A simple algorithm for regional analysis studies, *Res. Rep. Ser., 2005/1*, Univ. of Minn. Supercomputing Inst., Minneapolis. (Available at http://www.msi.umn.edu/cgi-bin/reports/searchv2.html)

Dutnell, R. C. (2000), Development of bankfull discharge and channel geometry relationships for natural channel design in Oklahoma using a fluvial geomorphic approach, M.S. thesis, Univ. of Okla., Norman.

Gupta, V. K. (2004), Emergence of statistical scaling in floods on channel networks from complex runoff dynamics, *Chaos Solitons Fractals*, *19*, 357–365.

Gupta, V. K., and E. Waymire (1990), Multiscaling properties of spatial rainfall and river flow distributions, *J. Geophys. Res.*, *95*(D3), 1999–2009.

Gupta, V. K., O. J. Mesa, and D. Dawdy (1994), Multiscaling theory of floods: Regional quantile analysis, *Water Resour. Res.*, *30*(12), 3405–3421.

Knighton, D. (1984), *Fluvial Forms and Processes*, Edward Arnold, London.

Leopold, L. (1994), *A View of the River*, Harvard Univ. Press, Cambridge, Mass.

Leopold, L. B., and T. Maddock (1953), The hydraulic geometry of stream channels and some physiographic implications, *U.S. Geol. Surv. Prof. Pap.*, *252*, 57 pp.

McCandless, T. L. (2003), Maryland stream survey: Bankfull discharge and channel characteristics of streams in the Allegheny plateau and the valley and ridge hydrologic regions, *Rep. CBFO-S03-01*, 33 pp., U.S. Fish and Wildlife Serv., Chesapeake Bay Field Off., Annapolis, Md.

Menabde, M., and M. Sivapalan (2001), Linking space-time variability of rainfall and runoff fields on a river network: A dynamic approach, *Adv. Water Resour.*, *24*(9), 1001–1014.

Menabde, M., S. E. Veitzer, V. K. Gupta, and M. Sivapalan (2001), Tests of peak flow scaling in simulated self-similar river networks, *Adv. Water Resour.*, *24*(9), 1037–1049.

National Water Management Center (2004), Osage Plains regional curves, Nat. Resour. Conserv. Serv., U.S. Dep. of Agric., Little Rock, Ark. (Available at http://wmc.ar.nrcs.usda.gov/technical/HHSWR/Geomorphic/)

Pandey, G. R. (1998), Assessment of scaling behavior of regional floods, *J. Hydrol. Eng.*, *3*(3), 169–173.

Perica, S., and E. Foufoula-Georgiou (1996), Linkage of scaling and thermodynamic parameters of rainfall: Results from midlatitude mesoscale convective systems, *J. Geophys. Res.*, *101*(D3), 7431–7448.

Prasad, L. (1997), Morphological analysis of shapes, *Rep. LALP-97-010-139, CNLS Newsl., 139*, Cent. for Nonlinear Stud., T-DOT, Theoret. Div., Los Alamos Natl. Lab., Los Alamos, N. M.

Richards, K. (1982), *Rivers: Form and Process in Alluvial Channels*, Methuen, New York.

Robinson, J. S., and M. Sivapalan (1997), An investigation into the physical causes of scaling and heterogeneity of regional flood frequency, *Water Resour. Res.*, *33*(5), 1045–1059.

Smith, J. A. (1992), Representation of basin scale in flood peak distributions, *Water Resour. Res.*, *28*(11), 2993–2999.

Williams, G. P. (1978), Bankfull discharge of rivers, *Water Resour. Res.*, *14*(6), 1141–1154.

Wolman, M. G., and J. P. Miller (1960), Magnitude and frequency of forces in geomorphic processes, *J. Geol.*, *68*, 54–74.

————————————

B. Dodov and E. Foufoula-Georgiou, National Center for Earth-Surface Dynamics, Department of Civil Engineering, University of Minnesota, Mississippi River at 3rd Avenue SE, Minneapolis, MN 55414, USA. (efi@umn.edu)